Development of Obstacle Avoidance Control System Using Modified Attractive Equations of Gaussian Potential Function

Kanapat Saenrit and Danai Phaoharuhansa*

Department of Mechanical Engineering, King Mongkut's University of Technology Thonburi, Bangkok, Thailand
Email: kanapat.saen@kmutt.ac.th (K.S.); danai.pha@kmutt.ac.th (D.P.)
*Corresponding author

***Abstract*—Navigation system is a necessary system for autonomous vehicle and many papers proposes the techniques for trajectory tracking and obstacle avoidance. Gaussian potential function is well-known for trajectory tracking control system with obstacle avoidance using 2D lidar. The disadvantage is that it relies on local minima, which is unable to deviate the moving path in some cases that vehicle and target is moving in the same direction, and obstacle is in between because the temptation of attractive potential field is too high. Then, the trajectory tracking control with obstacle avoidance using a modified attractive function has been introduced that conventional attractive function of gaussian potential function is modified in order to improve the navigation system. The simulation is performed by CARLA Simulator and the motion of the obstacle avoidance using the modified function is considered by the sway motion during the tracking and the safety during the lateral motion, which is considered by lateral acceleration of the vehicle, its value in simulation case is less than other types of attractive function. Meanwhile, the modified function also maintains the safety distance gap between the vehicle and the obstacle to not avoid at very close range from obstacle, which probably cause the collision.**

***Keywords*—trajectory tracking control system, obstacle avoidance, gaussian potential function, attractive function, CARLA Simulator**

I. Introduction

In recent years, autonomous vehicle technology has taken huge progress in order to overcome human behaviors and extenuate the danger such as road accidents [1], which is one of the main reasons of human death [2]. The navigation system is one of necessary systems, which guides the vehicle along the path to the destination by usage of real-time geographical environment [3]. It consists of three subsystems such as path planning, trajectory tracking control system [4] and obstacle avoidance control system [5–9]. It assists the driver to avoid the collision by traffic accident. Trajectory tracking control system is path tracking with time-varying states along the path, such as position, velocity, or orientation, which can be defined by a set of waypoints, functions, or sequences. It is a kind of feedback control system, which performs acceleration pedal, brake, and steering systems in order to track the path relative to distance and direction.

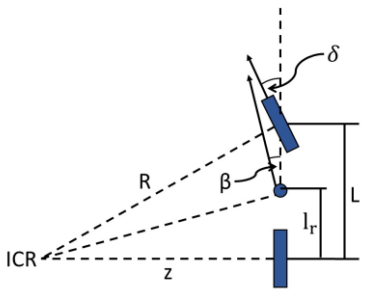

Fig. 1. Steering geometry of front-wheel steering.

One of popular methods of obstacle avoidance control system is potential field, which relies on attractive and repulsive field [6]. Many researchers tried to explore the knowledge about potential field method in order to avoid the obstacle. Artificial Potential Field (APF) technique [7–9] is well known technique for obstacle avoidance control system. It obtains the problem that the obstacle avoidance control system using APF cannot avoid the obstacle completely when the obstacle and target become close together [8, 9].

The Obstacle-Dependent Gaussian Potential Field (ODG-PF) method was developed to be an alternative method [10]. It is able to cover the problem of APF by creating attractive and repulsive equation for calculating at each heading angle to find local minima point [11–13]. ODG-PF still has problem in avoiding the obstacle in some cases such as when the vehicle and target is moving in the same direction with their alignment and the obstacle is in between. The attractive potential field, which normally is linear function, has strong temptation results in the deviation of the vehicle's moving path is ineffectively [14, 15]. Therefore, the purpose of this study aims to compare the attractive function and improve the

Manuscript received January 18, 2024; revised February 11, 2024; accepted March 18, 2024; published June 21, 2024.

function for obstacle avoidance control system of autonomous vehicle.

II. Dynamic Model

A. Bicycle Model

To consider the lateral motion of vehicle, four wheeled vehicle model is usually simplified to two wheeled vehicle model by assuming only front and rear wheels. Then, bicycle model is presented as the simple car model. Free-body-diagram and motion in any driving conditions are considered based on bicycle model.

Fig. 1 represents a front-wheel steering vehicle during lateral motion, the front wheel orientation can control the heading of the vehicle. The steering angle (δ) can be determined by Ackerman steering angle. It is given as expressed in Eq. (1):

$$\delta = L/R \tag{1}$$

where δ is steering angle, L is wheelbase length which is 3.632 m, and R is the distance between instantaneous center of rotation (ICR) and front wheel.

Then, the heading angle (β) can be expressed by

$$\beta = \tan^{-1}\left(\frac{l_r \tan\delta}{L}\right) \tag{2}$$

where l_r is the distance between the rear-wheel and center of gravity of the vehicle, which equals to 1.816 m, δ is steering angle, L is length of wheel base.

B. Rollover

The rollover or overturn is one of important indicators, which presents an emergency situation for lateral motion that the vehicle loses its stability. It causes fatal accidents on the road at a higher rate than any other type of road accident. Considering a vehicle's front-view free body diagram in Fig. 2, the unstable condition in a rollover situation, the force applied on the inside wheel is zero, can be considered by moment equilibrium as shown in Eq. (3):

$$-mg\frac{T}{2} + \left(m\frac{\dot{x}^2}{R}H + m\dot{\beta}H\right) = 0 \tag{3}$$

where, m is the mass of the vehicle, T is track width of the vehicle which is 2.027 m, H is the height of center of gravity of the vehicle, $\dot{x}$ is the velocity of the vehicle, R is the radius of curvature and $\dot{\beta}$ is the yaw rate.

From Eq. (3), the lateral acceleration is defined as

$$a_c = \frac{\dot{x}^2}{R} + \dot{\beta} \tag{4}$$

where a_c is lateral acceleration, $\dot{x}$ is the velocity of the vehicle, R is radius of curvature, and $\dot{\beta}$ is the yaw rate.

Then, replace Eq. (4) into Eq. (3). the maximum lateral acceleration ($a_{c,max}$) before the vehicle turnovers. The maximum lateral acceleration is given by

$$a_{c,max} = \frac{gT}{2H} \tag{5}$$

where $a_{c,max}$ is the maximum lateral acceleration of vehicle, g equals to 9.81 m/s^2, T is track width of the vehicle, H is the height of center of gravity.

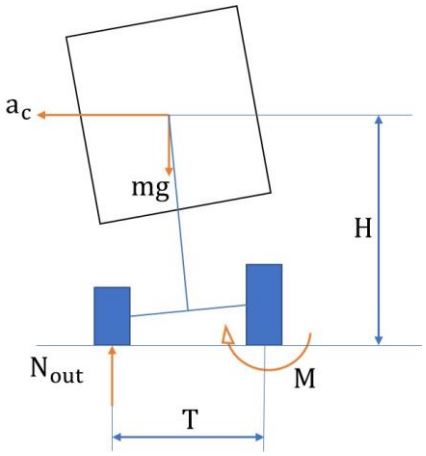

Fig. 2. Free-body diagram of vehicle in front view.

III. Trajectory Tracking Control System with Obstacle Avoidance

Trajectory tracking control system is used to navigate the vehicle to the destination through thetrajectory that is provided by set of waypoint between the vehicle and the destination. This function can collaborate with other function to give some additional instructions to the vehicle, and one of them is obstacle avoidance control which is the function that has the environment parameter to detect obstacles in order to adjust the path of movement to avoid the collision.

A. Obstacle-Dependent Gaussian Potential Function

Obstacle-Dependent Gaussian Potential Function (ODG-PF) is designed based on attractive function and repulsive function. Then, this section will describe both functions as follows.

1) Attractive potential function

The attractive potential field is the virtual force that guides a vehicle to its destination. The global position in the local vehicle system is unknown and the initial direction that is generally set to the vehicle's moving direction is defined. From the initial position, the vehicle is able to return to the expected global position after escaping the obstacle.

The attractive function has been modified by combining the linear and exponential functions as shown in Eq. (9). Then, it is compared with the conventional functions such as linear function, parabola function, and exponential function, respectively. They are shown in Eqs. (6)–(8), subsequently.

$$f_{att,l}(\theta_i) = \gamma_l|\Delta\theta_i| \tag{6}$$

$$f_{att,p}(\theta_i) = \gamma_p(\Delta\theta_i)^2 \tag{7}$$

$$f_{att,e}(\theta_i) = \gamma_e^{|\Delta\theta_i|} \tag{8}$$

$$f_{att,c}(\theta_i) = \gamma_{cl}|\Delta\theta_i| + \gamma_{ce}^{|\Delta\theta_i|} \quad (9)$$

where $f_{att,l}$, $f_{att,p}$, $f_{att,e}$, $f_{att,c}$ are linear, parabora, and modified attractive potential value in domain of angle (θ), respectively. γ_l, γ_p, γ_e, γ_{cl}, and γ_{ce} denote the constant value for potential function which are determined as 1.8, 0.03, 1.08, 0.8, and 1.07 subsequently.

2) Repulsive potential function

The repulsive potential field is the virtual force that relies on distance and the corresponding angle of each obstacle. It is used to push the vehicle out of the obstacle.

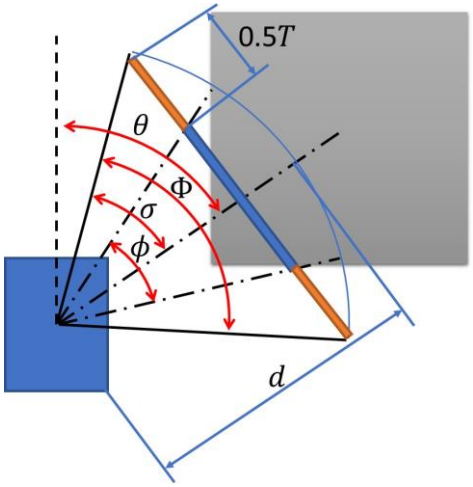

Fig. 3. Corresponding angle of the obstacle.

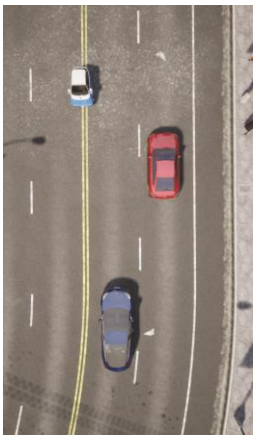

(a)

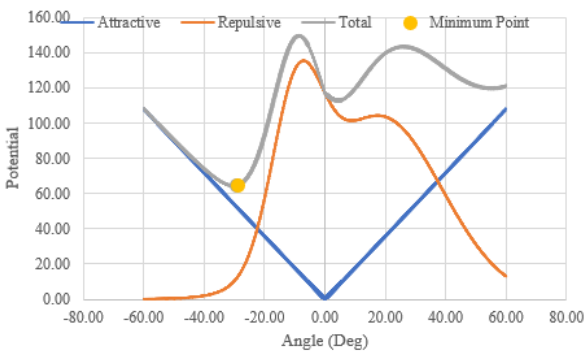

(b)

Fig. 4. Obstacle detection: (a) Vehicle with two obstacles in front; (b) Total potential and local minimum point.

In obstacle avoidance application, the width of the vehicle should also be considered in the calculation as expressed in Fig. 3; therefore, half of vehicle's width is added to each ending of the detected obstacle to ensure safe avoidance.

$$\Phi_k = 2\sigma_k = 2\tan^{-1}\left(\frac{d_k \tan\frac{\phi_k}{2} + \frac{T}{2}}{d_k}\right) \quad (10)$$

where Φ_k is the sweep angle with half of vehicle's width. σ_k is the angle between the center of obstacle and the edge of obstacle. d_k is the distance between the obstacle and the vehicle. ϕ_k is the original sweep angle of obstacle, T is track width of the vehicle.

The difference between the distance of obstacle and maximum detection distance can be called inverse distance as shown in Eq. (11)

$$\tilde{d}_k = d_{max} - d_k \quad (11)$$

where $\tilde{d}_k$ is inverse distance, d_{max} is maximum detection distance, d_k is the distance of obstacle.

The repulsive potential field is obtained from summing all gaussian likelihood functions of obstacles.

$$f_{rep}(\theta_i) = \sum_{k=1}^{n} \tilde{d}_k \exp\left(\frac{1}{2}\right) \exp\left(-\frac{(\theta_k - \theta_i)^2}{2\sigma_k^2}\right) \quad (12)$$

where f_{rep} is the repulsive potential. θ_k is the angle at the center of the obstacle. θ_i is the calculating angle, and σ_k is the angle between the center and edge of the obstacle.

The total potential field is calculated by adding the attractive and repulsive fields together. The local minimum value of total potential is defined by the yellow dot in Fig. 4(b), which is probably the moving angle to avoid all obstacles safely.

IV. CARLA Simulator

In autonomous vehicle control simulation, the program and algorithm are normally tested in the simulation program first to reduce the increase in unnecessary damage costs or unexpected accidents. The selected program is CARLA, an open-source simulator based on Unreal Engine for autonomous driving research. CARLA was developed to support the development, training, and validation of autonomous driving systems. The open digital environment (urban layouts, buildings, vehicles) is also available and can be used freely. The simulation platform supports flexible specification of sensors and environmental conditions.

1) Environment system & map

CARLA simulation program is used to simulate the vehicle motion. It is a set of default maps available for the user to simulate in defined situations. For this research, a square map with some crossroad, as shown in Fig. 5, is sufficient to cover the scenario case.

2) Scenario case & boundary conditions

For the simulation scenario as provided in Fig. 6, two vehicles will be spawned in the map, one is a testing

vehicle and the other is an obstacle vehicle with a distance of 20 m. The obstacle vehicle is offset from the testing vehicle by 0.5 m and stays at the same position. The destination is defined at 70 m straight from the testing vehicle. The target of the simulation is testing vehicle has to move pass obstacle vehicle without collision whether a function will be used as an attractive potential function.

Fig. 5. Default map in CARLA Simulator.

Fig. 6. Scenario case.

V. Simulation Result and Discussion

In the simulation, three attractive functions will be used to compare the behavior, path, and other parameters. To make a clear comparison, the combination between linear and exponential functions is included, so in total of four functions. The result of total potential functions has been illustrated in Fig. 7, respectively.

The parameter and specification of vehicle in this research comes from the real-car model to get the result as close as the reality, and the selected vehicle is Tesla Model 3, The constant and exponential base of parabola, exponential, and combination of linear and exponential attractive potential field in Eqs. (7)–(9), respectively. They are adjusted by considering at both side of maximum heading angle that vehicle can turn, then adjust the value of potential field to equal with value from linear potential field.

According to the results, the vehicle control parameter is local minima of the resultant potential field as shown in Fig. 7 and Table I, the minimum value angle for each type of attractive function is −19.90°, −21.62°, −25.51°, and −22.40°, respectively. However, the parameter that effects the local minima is not the value, but the slope of the attractive function, so the local minima of exponential function can reach furthest among all three.

The avoidance duration approximately occurs at time about 0.5–5 s. During that time, the heading angle is higher than other time as expressed in Fig. 8. The exponential function has highest heading angle around 35° at time 3.25 s. At time about 5.5–7 s, it reveals short time turn left before returning to the original path of the vehicle.

TABLE I. Minimum Total Potential Angle at Initial Position

Function	Minimum Potential Angle
Linear	−19.90°
Parabola	−21.62°
Exponential	−25.51°
Linear + Exponential	−22.40°

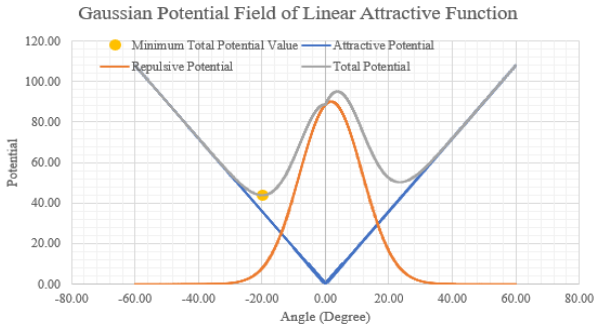

(a)

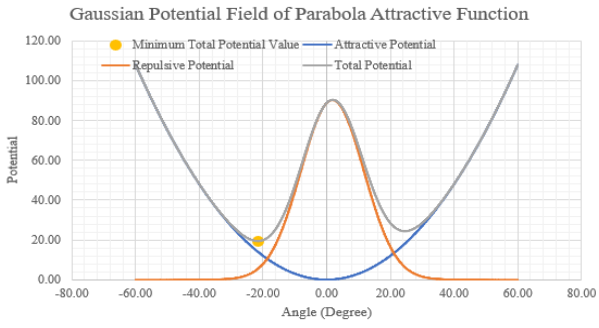

(b)

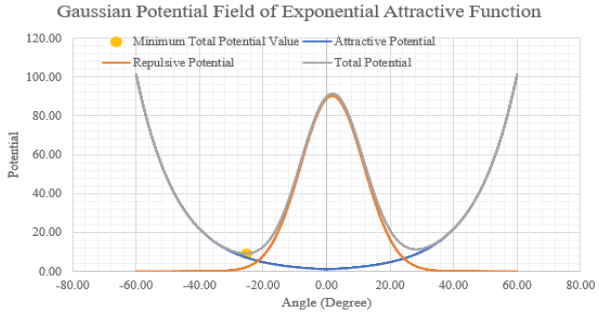

(c)

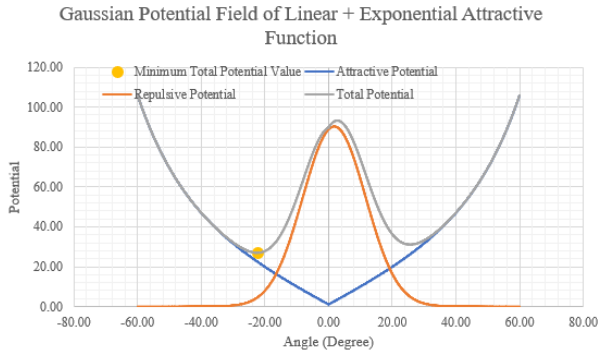

(d) Modified Attractive Function

Fig. 7. Total potential field at the initial position: (a) linear attractive function; (b) parabola attractive function; (c) exponential attractive function; (d) modified attractive function.

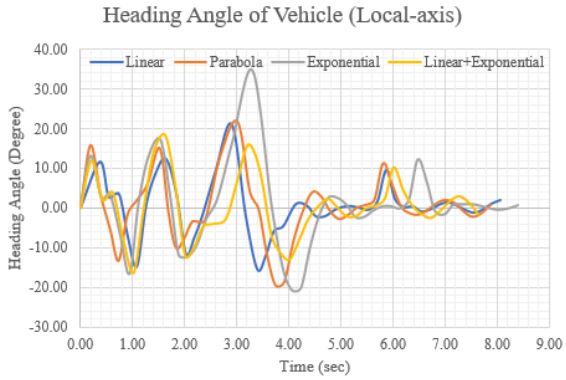

Fig. 8. Heading angle of the testing vehicle.

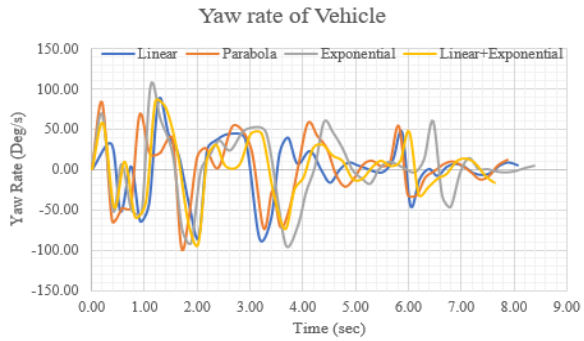

Fig. 9. Yaw rate of the testing vehicle.

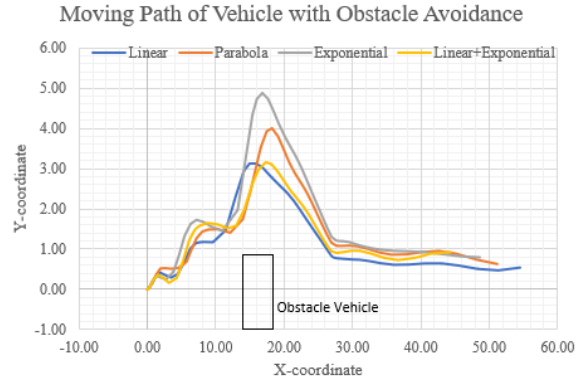

Fig. 10. Moving path of the testing vehicle.

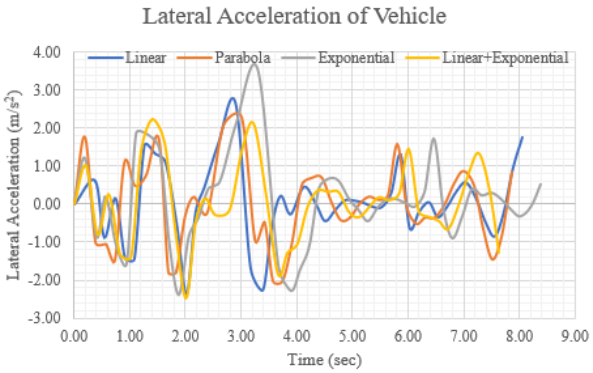

Fig. 11. Lateral acceleration of the testing vehicle.

After that, the lateral acceleration can be calculated by using yaw rate from Fig. 9 by Eqs. (1), (2), and (4), the lateral acceleration is illustrated in Fig. 11, which can be used as a rollover indicator. The value at any time interval must not exceed the constant in Eq. (5) in order to maintain the stability on rotation around x-axis. The exponential function has highest value around 3.70 m/s^2 at time 3.20 s. Therefore, it has probability to reach rollover situation first if the velocity of vehicle is increased.

To consider the avoidance performance, the main factors consist of three main factors. The distance gap as shown in Fig. 10 indicates risk of collision risk indicator. The sway of the vehicle has been presented by the yaw rate to determine the stability and smoothness of the avoidance as shown in Fig. 9. All types of potential field are in the same trend with similar value. The lateral acceleration in Fig. 11 is important as similar as the distance gap because it can determine the rollover situation following Eq. (4) the rollover in this simulation occurs when lateral acceleration in Eq. (5) exceed 15.657 m/s^2.

As summary, each type of attractive potential field is enumerated by considering the path deviation, collision risk, and turning behavior shows that the linear potential field is the most conservative function because the slope of attractive function in Eq. (6) around current heading angle is 1.8 deg^{-1}, which is highest. It effects to maintain the original path until it reaches some position, and the vehicle rapidly avoids the obstacle. Although the heading angle is not high but lateral acceleration is increased. The parabola potential field is less conservative function than linear because the attractive slope of Eq. (7) around current heading angle is only 0.75 deg^{-1}. The vehicle starts to avoid earlier than linear to prevent the rapid turning. Then, the lateral acceleration remains 85.71% from linear function. The exponential function obtains lowest collision risk, but the vehicle tries to turn early with high value of heading angle. Thus, the vehicle occurs the sharp turn to back the original path and the sway of vehicle are also high that the lateral acceleration with exponential attractive field is 132.14% from linear attractive field.

The modified function expectation performs the new path as linear and it has low collision risk as exponential function because high path deviation probably causes another collision risk circumstances, and the sharp turn should be vanished. The results in Fig. 10 present that

modified function turns earlier, which confirms low risk of collision while the path deviation is not different from linear function as much as exponential function do. Moreover, the sway motion and lateral acceleration is explicitly about 2.5–4.5 s. The modified function has the good ability to cover the main disadvantages of Gaussian Potential Field because it reduces the temptation of attractive potential by reducing the slope around current heading angle.

VI. Conclusion

This research is about the comparison of three types of attractive function, linear function, parabola function, and exponential function, with a combination of linear and exponential functions is also included.

The behavior of vehicle for each type of attractive function is slightly different in terms of lateral acceleration and yaw rate which linear and modified function has better control capability and stability, however, the linear function has more rigid consideration and avoidance that makes the distance gap between a vehicle and an obstacle is too close and risk of collision while modified function can deviate a moving path to better distance gap.

Comparison between parabola and exponential functions is that the two functions have ability to deviate the path more than other two because of their potential slope in low angle range. However, the stability, and lateral acceleration are the exchange of safety distance gap that is higher, especially the exponential function which its lateral acceleration is the highest among all functions. Therefore, the exponential function must be most cautious in terms of rollover conditions.

Conflict of Interest

The authors declare no conflict of interest.

Author Contributions

Conceptualization, K.S. and D.P.; methodology, K.S.; software, K.S. and D.P.; validation, K.S.; formal Analysis, K.S. and D.P.; investigation, D.P.; resources, D.P.; data curation, K.S.; writing-original draft preparation, K.S.; writing-review and editing, K.S. and D.P.; visualization, K.S.; supervision, D.P.; all authors had approved the final version.

Funding

This research has received funding support from the National Science, Research and Innovation Fund (NSRF) via the Program Management Unit for Human Resources & Institutional Development, Research and Innovation [grant number B40G660039].

References

[1] M. Martínez-Díaz and F. Soriguera, "Autonomous vehicles: Theoretical and practical challenges," *Transportation Research Procedia*, vol. 33, pp. 275–282, 2018. https://doi.org/10.1016/j.trpro.2018.10.103

[2] H. Wang, Y. Huang, A. Khajepour, Y. Zhang, Y. Rasekhipour, and D. Cao, "Crash mitigation in motion planning for autonomous vehicles," *IEEE Transactions on Intelligent Transportation Systems*, vol. 20, no. 9, pp. 3313–3323, Sept. 2019. doi: 10.1109/TITS.2018.2873921

[3] W. Rahiman and Z. Zainal, "An overview of development GPS navigation for autonomous car," in *Proc. 2013 IEEE 8th Conference on Industrial Electronics and Applications (ICIEA)*, Melbourne, VIC, Australia, 2013, pp. 1112–1118. doi: 10.1109/ICIEA.2013.6566533

[4] N. Hassan and A. Saleem, "Analysis of trajectory tracking control algorithms for wheeled mobile robots," in *Proc. 2021 IEEE Industrial Electronics and Applications Conference (IEACon)*, Penang, Malaysia, 2021, pp. 236–241. doi: 10.1109/IEACon51066.2021.9654675

[5] Y. Fujiwara and S. Adachi, "Control system design for obstacle avoidance system using model predictive control," in *Proc. the 2004 IEEE International Conference on Control Applications*, Taipei, Taiwan, 2004, pp. 1591–1596, vol. 2. doi: 10.1109/CCA.2004.1387603

[6] Y. Koren and J. Borenstein, "Potential field methods and their inherent limitations for mobile robot navigation," in *Proc. 1991 IEEE International Conference on Robotics and Automation, Sacramento*, CA, USA, 1991, vol. 2, pp. 1398–1404. doi: 10.1109/ROBOT.1991.131810

[7] I. Iswanto, A. Ma'arif, O. Wahyunggoro, and A. I. Cahyadi, "Artificial potential field algorithm implementation for quadrotor path planning," *International Journal of Advanced Computer Science and Applications (IJACSA)*, vol. 10, no. 8, 2019. http://dx.doi.org/10.14569/IJACSA.2019.0100876

[8] Q. Zhu, Y. Yan, and Z. Xing, "Robot path planning based on artificial potential field approach with simulated annealing," in *Proc. Sixth International Conference on Intelligent Systems Design and Applications*, Jian, China, 2006, pp. 622–627. doi: 10.1109/ISDA.2006.253908

[9] L. Tang, S. Dian, G. Gu, K. Zhou, S. Wang, and X. Feng, "A novel potential field method for obstacle avoidance and path planning of mobile robot," in *Proc. 2010 3rd International Conference on Computer Science and Information Technology*, Chengdu, 2010, pp. 633–637. doi: 10.1109/ICCSIT.2010.5565069

[10] D. Phaoharuhansa, N. Supperm, K. Raksawid, and C. Kampeewichean, "Obstacle avoidance system using 2d lidar for autonomous vehicle," presented at Asia Pacific Conference on Robot IoT System Development and Platform 2022 (APRIS 2022), Tokyo, November 1–2, 2022.

[11] J. H. Cho, D. S. Pae, M. T. Lim, and T. K. Kang, "A real-time obstacle avoidance method for autonomous vehicles using an obstacle-dependent Gaussian potential field," *Hindawi Journal of Advanced Transportation*, pp. 4–6, August 2018. https://doi.org/10.1155/2018/5041401

[12] D. Kim, D. Lee, J. Oh, T. H. Kang, and T. K. Kang, "Local obstacle avoidance using obstacle-dependent Gaussian potential field for robot soccer." *Robot Intelligence Technology and Applications*, vol. 4, pp. 539–549, July 2016. https://doi.org/10.1007/978-3-319-31293-4_44

[13] D.-S. Pae, G.-H. Kim, T.-K. Kang, M.-T. Lim, "Path planning based on obstacle-dependent Gaussian model predictive control for autonomous driving," *Applied Sciences*, vol. 11, no. 8, 3703, 2021. https://doi.org/10.3390/app11083703

[14] S. Ge and Y. Cui, "Dynamic motion planning for mobile robots using potential field method," *Autonomous Robots*, vol. 13, pp. 207–222, 2002. https://doi.org/10.1023/A:1020564024509

[15] Z. Xu, R. Hess, and K. Schilling, "Constraints of potential field for obstacle avoidance on car-like mobile robots," *IFAC Proceedings Volumes*, vol. 45, issue 4, pp. 169–175, 2012. https://doi.org/10.3182/20120403-3-DE-3010.00077